

## Research Article

# Growth and Characterization of Agar Gel Grown Brushite Crystals

**V. B. Suryawanshi and R. T. Chaudhari**

*Physics Research Lab, Shri. V. S. Naik Arts, Commerce and Science College, Raver 425508, India*

Correspondence should be addressed to V. B. Suryawanshi; [vbsuryawanshi2007@rediffmail.com](mailto:vbsuryawanshi2007@rediffmail.com)

Received 27 October 2013; Accepted 2 December 2013; Published 8 January 2014

Academic Editors: A. Cremades and A. D. Yadav

Copyright © 2014 V. B. Suryawanshi and R. T. Chaudhari. This is an open access article distributed under the Creative Commons Attribution License, which permits unrestricted use, distribution, and reproduction in any medium, provided the original work is properly cited.

Brushite [ $\text{CaHPO}_4 \cdot 2\text{H}_2\text{O}$ ] or calcium hydrogen phosphate dihydrate (CHPD) also known as urinary crystal is a stable form of calcium phosphate. The brushite crystals were grown by single and double diffusion techniques in agar-agar gel at room temperature. Effects of different growth parameters were discussed in single diffusion and double diffusion techniques. Good quality star, needle, platy, rectangular, and prismatic shaped crystals in single diffusion and nuclei with dendritic growth were obtained in double diffusion. These grown nuclei were characterized by scanning electron microscopy (SEM), Fourier transform infrared (FTIR) spectroscopy, X-ray diffraction (XRD), and thermogravimetric analysis (TGA). SEM has shown the different morphologies of crystals; FTIR has confirmed the presence of functional groups; crystalline nature was supported by XRD, whereas the TGA indicates total 24.68% loss in weight and formation of stable calcium pyrophosphate ( $\text{Ca}_2\text{P}_2\text{O}_7$ ) at  $500^\circ\text{C}$ .

## 1. Introduction

Calcium oxalates, phosphates, and their hydrates are very common in calcium renal stones. Some of the oxalates are found in either pure or in mixed form with phosphate and also reported with uric acid or ammonium urates [1, 2]. Calcium oxalate monohydrate [3, 4] and calcium oxalate dihydrate [5] are common constituents of calcium urinary crystal while hydroxypatite [6], carbonate apatite [7], and brushite [8–11] are in calcium phosphate crystals. Brushite [ $\text{CaHPO}_4 \cdot 2\text{H}_2\text{O}$ ] provides a medium to grow octacalcium phosphate [12] and hydroxypatite [13–16] urinary crystals, however used as a precursor to form apatite, which has an important application in bone formation [17, 18].

Gel method is the most versatile and simple technique for growing urinary crystals [19–21]. In this method, gel acts as an inert and viscous medium for the growth of these crystals [22, 23].

The growth inhibition study of brushite crystals are reported in silica gel by adding tamarind, tartaric acid, and citric acid [24, 25] and in the presence of sodium fluoride [26]. Lim et al. [27] have grown three-dimensional flower like brushite crystals from high internal phase emulsion

processing route; whereas Kumar and Kalainathan [28] have grown in the presence of magnetic field and observed the effect on growth of these crystals. Parekh et al. [29] have also observed the growth inhibition and dissolution of urinary type micro-CHPD crystals. Most of the brushite crystals reported are grown in silica hydrogel; however the growth of these crystals is not reported in agar-agar gel.

In the present work, the brushite crystals were grown in agar-agar gel at ambient temperature and were characterized by scanning electron microscopy (SEM), Fourier transform infrared (FTIR) spectroscopy, X-ray diffraction (XRD), and thermogravimetric analysis (TGA).

## 2. Experimental

In the present study, brushite crystals were grown by single and double diffusion techniques [30]. In this method, glass test tubes of size 15 cm in length and 1.8 cm in diameter and U-tube of size 25 cm in length and 2.5 cm in diameter were used as crystallization vessels. Agar gel (Himedia) solution was prepared by the mixing (0.25 to 1.0 gm) of agar powder in 100 mL double distilled water at boiling temperature. Potassium dihydrogen phosphate (KDP) (Merck) of concentration



FIGURE 1: Brushite crystals with controlled nucleation in single diffusion.

TABLE 1: Optimum conditions for the growth of brushite crystals.

Condition	Single diffusion	Double diffusion
% of gel	0.5	1.0
Con. of calcium chloride	1 M	1 M
Con. of KDP	1 M	1 M
Gel setting period	24 hrs	24 hrs
Gel aging	48 hrs	48 hrs
Period of growth	60 days	80 days
Temperature	Room temp.	Room temp.
Quality	Transparent	Opaque
Shape	star, needle, platy, rectangular, and prismatic shaped	Dendritic shaped

0.5–1.0 M and calcium chloride (Qualigens) of concentration 0.5–1.0 M were used as reactants.

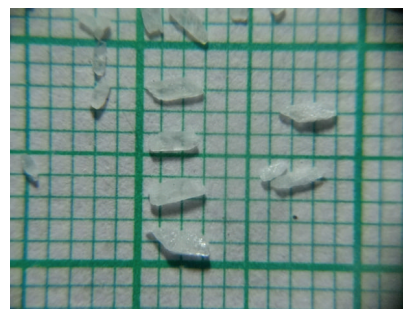
For single diffusion techniques, the agar solution was mixed with the desired concentration and appropriate volume of calcium chloride. After setting and aging of gel, an aqueous solution of KDP was poured over the gel. No precipitation was observed; however after 1–8 days, nucleation was seen at the interstitial and inside the gel.

The same method was repeated by reversing the reactants. But no nucleation was observed in this method.

In double diffusion, agar solution was poured in U tube up to appropriate height. After setting and aging of gel, an aqueous solution of KDP was poured in one limb, while in other limb an aqueous solution of calcium chloride was poured over the gel. As both the solutions diffused in the gel, nucleation was observed after 10 days. This nucleation was further increased and took two months for its complete growth. After two months, well-shaped brushite crystals were grown inside the gel as shown in Figure 2.



(a)



(b)



(c)

FIGURE 2: Harvested star, needle, platy, rectangular, and prismatic shape brushite crystals.

These grown crystals were harvested from test tubes and were characterized by, SEM, FTIR, XRD, and TGA.

### 3. Result and Discussion

**3.1. Growth.** In single diffusion technique, many researchers [9, 17, 31] have observed Liesegang ring phenomena in silica gel; however no Liesegang ring phenomena is observed in the present study. After diffusion of supernatant in the gel, heavy nucleation was observed. To control nucleation various parameters such as concentration of gel, concentration of reactant, aging of gel, and volume of reactants were changed, which can be seen in Figure 1, and thus optimum conditions are established as shown in Table 1. Figure 2 shows some good quality star, needle, and transparent prismatic platy shaped crystals grown in single diffusion.

In double diffusion technique, nucleation was started after diffusion of both reactants in gel. This growth can be seen in Figure 3, and their optimum conditions are

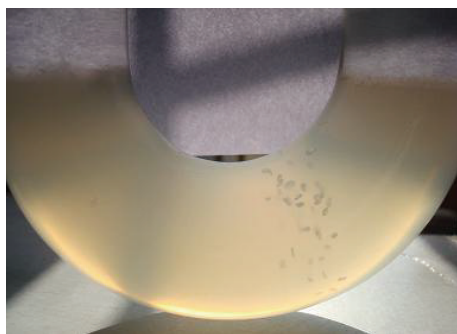


FIGURE 3: Growth of brushite crystal in double diffusion.



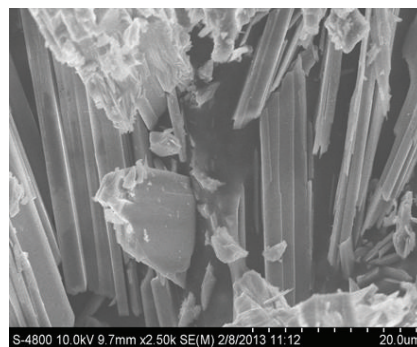
(a)



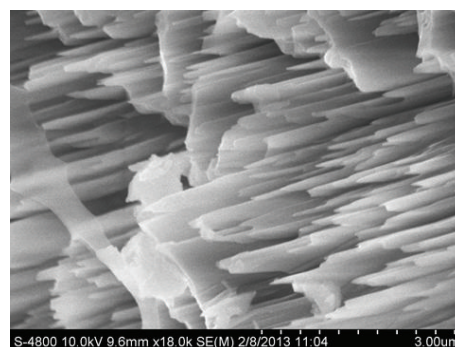
(b)

FIGURE 4: 20X image of brushite crystals grown in double diffusion (a) dendritic shaped (b) edge growth.

shown in Table 1. Interesting phenomenon was observed in case of crystals grown in double diffusion. After formation of crystals, the growth was again started from edges and found in dendritic shape. Figure 4(a) shows the 20X image of dendritic shaped brushite crystals in double diffusion. Figure 4(b) shows that a bulk nucleus is surrounded by several tiny nuclei at the interstitial, but not at the centre. This one can be easily understood by considering free energy changes associated with the formation of nuclei, and association of several tiny nuclei at the edges may be due to the reason that the surface molecules are less well bound to their neighbors than are those in bulk [32].



(a)



(b)

FIGURE 5: SEM images of brushite crystals: (a) plate shaped and (b) crowded rod shaped morphology.

### 3.2. Characterization

**3.2.1. Scanning Electron Microscopy.** The morphology of the crystals can be observed by SEM as shown in Figures 5(a) and 5(b). These figures show that the crystals are platy shaped and crowded by making some angles with c-axis. In Figure 5(a), microrectangular plate shape placed over the other morphology can be seen. Whereas Figure 5(b) shows that rods are inclined and crowded. The reason of formation of platy shape may be due to the growth of crystals in two dimensions.

**3.2.2. Fourier Transform Infrared Spectroscopy.** Figure 6 shows the recorded FTIR spectrum of brushite crystal.

The absorption peaks at  $3541.42\text{ cm}^{-1}$  [33, 34] and  $3151.79\text{ cm}^{-1}$  [9] are attributed to O–H stretching. The peak at  $1649.19\text{ cm}^{-1}$  [35] is assigned to that of O–H bending, whereas the weak absorptions at  $2395.67$  and  $1766.85$  are associated to  $\text{HPO}_4^{2-}$  [9], while stretching vibrations associated with P=O were observed at  $1215.19$ ,  $1126.47$ , and  $1062.81\text{ cm}^{-1}$  [17]. The P–O–P asymmetric stretching vibrations give rise to absorptions at  $987.59$ ,  $862.21$ , and  $808.20\text{ cm}^{-1}$  [17]. Two bands at  $580.59$  and  $520.80\text{ cm}^{-1}$  are due to acid phosphate (H–O–) P=O bond vibration [17, 36]. FTIR spectroscopy confirmed the growth of brushite crystals due to the presence of water of crystallization, P=O bond, and O–H bond [9]. The assigned vibrations with observed wave numbers are given in Table 2.



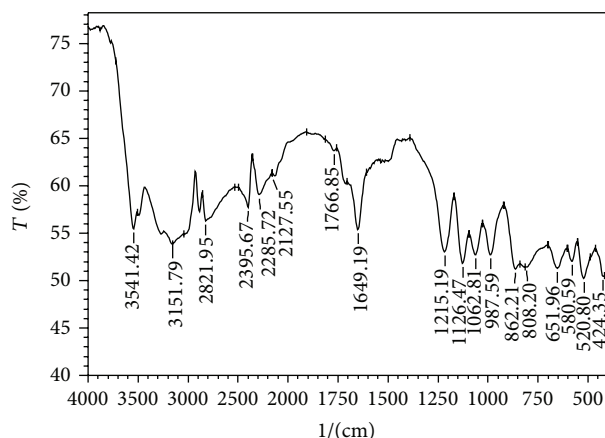


FIGURE 6: FTIR spectrum of brushite crystals.

TABLE 2: FTIR wave numbers and vibrations assignment of brushite crystal.

Sr. no.	Observed wave number in $\text{cm}^{-1}$	Bonds/vibrational assignments
1	3541.42	O–H stretching of water
2	3151.79	O–H stretching of water
3	2395.67	Weak absorption $\text{HPO}_4^{2-}$
4	1766.85	Weak absorption $\text{HPO}_4^{2-}$
5	1649.19	H–O–H symmetric bending vibrations
6	1215.19	$\text{PO}_4$ P=O associated stretching vibrations
7	1126.47	$\text{PO}_4$ bond, P=O stretching vibrations
8	1062.81	$\text{PO}_4$ bond, P=O stretching vibrations
9	987.59	P–O–P asymmetric stretching bond
10	862.21	P–O–P asymmetric stretching bond
11	808.20	P–O–P asymmetric stretching bond
12	580.59	(H–O–) P=O bond acid phosphate
13	520.80	(H–O–) P=O bond acid phosphate

**3.2.3. X-Ray Diffraction.** The X-ray diffractogram of the gel grown brushite crystal is shown in Figure 7. The crystalline phases and  $d$ -values obtained from the XRD pattern have been compared with those in the JCPDS data. The XRD pattern of Figure 7 matched with the JCPDS files [37, 38], indicating that the sample consisted of brushite crystalline. Table 3 gives the position,  $d$ -values, and matching peaks of the brushite crystals. Figure 8 shows plot identified phases of brushite crystal.

**3.2.4. Thermogravimetry.** Figure 9 shows the thermogram of brushite crystals recorded in the temperature range 50–710°C at the rate of 10.00°C/min. The curve shows weight loss in two stages. First stage is dehydration of brushite crystals. It has been observed that 35% of hydration of brushite is lost between 75°C to 125°C, and 59% and is lost from 125°C to 200°C, whereas 6% is lost from 200°C to 300°C. The total dehydration is done between 100°C and 300°C. Based upon

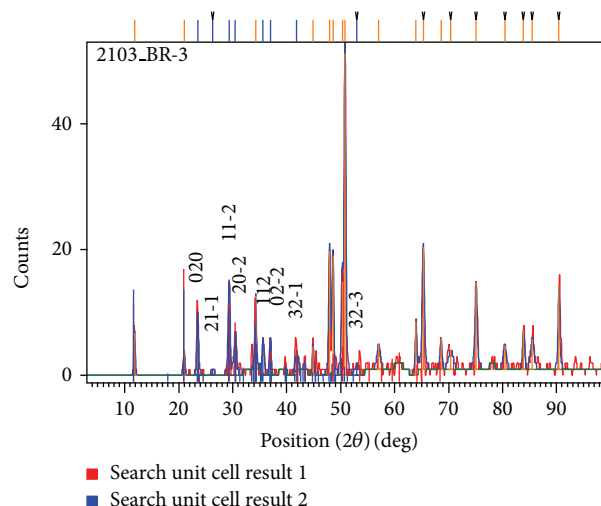


FIGURE 7: Powder diffractogram of brushite crystals.

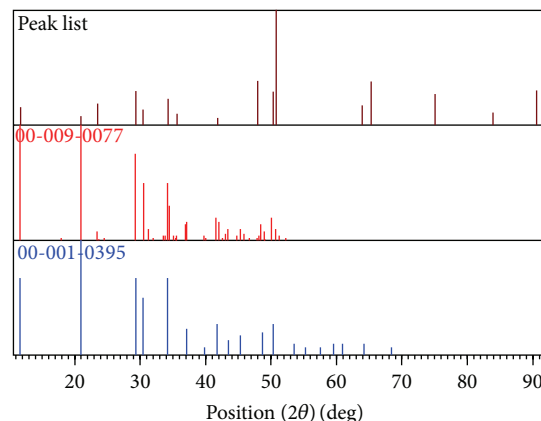


FIGURE 8: Plot of identified phases of brushite crystals.

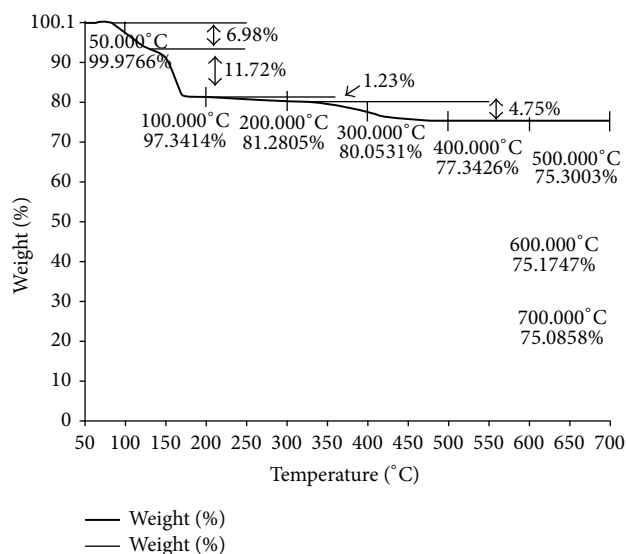
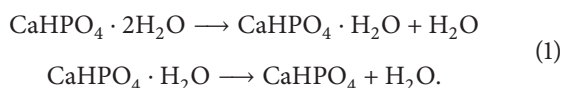


FIGURE 9: Thermogram of brushite crystals.

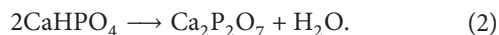
TABLE 3: The XRD data of brushite crystal.

Pos. (2 $\theta$ ) (deg)	Height (cts)	FWHM (2 $\theta$ ) (deg)	<i>d</i> -spacing (Å)	Rel. int. (%)	Matched by
11.7472	7.91	0.2952	7.52726	15.48	001-0395 [37]; 009-0077 [38]
20.9844	4.13	0.2952	4.23006	8.07	001-0395 [37]; 009-0077 [38]
23.5421	9.55	0.2952	3.77594	18.69	009-0077 [38]
29.3470	15.26	0.3444	3.04092	29.85	001-0395 [37]; 009-0077 [38]
30.4833	7.03	0.3936	2.93012	13.75	001-0395 [37]; 009-0077 [38]
34.2373	11.61	0.2952	2.61693	22.72	001-0395 [37]; 009-0077 [38]
35.6589	4.96	0.5904	2.51580	9.70	009-0077 [38]
41.8101	3.15	0.5904	2.15879	6.17	001-0395 [37]; 009-0077 [38]
47.9518	19.64	0.2952	1.89564	38.43	009-0077 [38]
50.3254	14.82	0.2952	1.81166	28.99	001-0395 [37]; 009-0077 [38]
50.8203	51.11	0.2952	1.79517	100.00	009-0077 [38]
63.9728	8.74	0.2952	1.45417	17.10	001-0395 [37]

the formula of brushite, the theoretical mass loss for the dehydration of brushite is 20.93% [39]. The observed mass loss for the dehydration of brushite crystals due to the first three steps is 19.93%. The following reaction is expected during the complete dehydration of brushite crystals and formation of monocyte [17, 39]:



In the second stage, at higher temperature between 300°C to 500°C, two molecules of  $\text{CaHPO}_4$  combine and result in the decomposition that occurs with the elimination of water molecules, leading to the formation of calcium pyrophosphate ( $\text{Ca}_2\text{P}_2\text{O}_7$ ) [9, 17, 39], and then the sample remains stable up to 75%. The theoretical mass loss for this step is 5.2% [39], where as the observed mass loss is 4.75%. A possible reaction for the decomposition and formation of calcium pyrophosphate is



#### 4. Conclusions

The brushite crystals were grown by single and double diffusion techniques using agar-agar gel as a medium of growth. Different morphologies, namely, star, platy, rectangular and prismatic shapes in single diffusion and dendritic growth in double diffusion were obtained. The presence of various functional groups is confirmed by FTIR spectroscopy. X-ray diffraction spectra have confirmed the crystalline nature. The proposed chemical formula and crystal structure for the grown sample are in good agreement with the results obtained from TGA studies.

#### Conflict of Interests

The authors declare that there is no conflict of interests regarding the publication of this paper.

#### Acknowledgments

The authors are thankful to the Principal of Shri V. S. Naik Arts, Commerce and Science College, Raver (M. S.), for providing laboratory facilities, thankful to Dr. P. V. Dalal, Shri V. S. Naik College, Raver, for fruitful discussion, and thankful to the Director of SICART (Gujarat) for providing characterization facilities.

#### References

- [1] A. Trinchieri, C. Castelnovo, R. Lizzano, and G. Zanetti, "Calcium stone disease: a multiform reality," *Urological Research*, vol. 33, no. 3, pp. 194–198, 2005.
- [2] R. B. Doddametkurke, S. B. Chandra, J. Anthony, and C. J. J. Browning, "The role of Urinary Kidney Stone inhibitors and promoters in the pathogenesis of calcium containing renal stones," *European Association Urology*, vol. 5, pp. 126–136, 2007.
- [3] D. Valarmathi, L. Abraham, and S. Gunasekaran, "Growth of calcium oxalate monohydrate crystal by gel method and its spectroscopic analysis," *Indian Journal of Pure and Applied Physics*, vol. 48, no. 1, pp. 36–38, 2010.
- [4] E. K. Girija, G. R. Sivakumar, S. Narayana Kalkura, P. Ramasamy, D. R. Joshi, and P. B. Sivaraman, "Knoop microhardness studies of urinary calculi and pure calcium oxalate monohydrate crystals," *Materials Chemistry and Physics*, vol. 63, no. 1, pp. 50–54, 2000.
- [5] M. S. Ansari, N. P. Gupta, A. K. Hemal et al., "Spectrum of stone composition: structural analysis of 1050 upper urinary tract calculi from northern India," *International Journal of Urology*, vol. 12, no. 1, pp. 12–16, 2005.
- [6] B. Parekh, M. Joshi, and A. Vaidya, "Characterization and inhibitive study of gel-grown hydroxyapatite crystals at physiological temperature," *Journal of Crystal Growth*, vol. 310, no. 7–9, pp. 1749–1753, 2008.
- [7] M. Menon, B. G. Parulkar, and G. W. Drach, "Urinary lithiasis, etiology, diagnosis and management," *Campbell's Urology*, vol. 3, pp. 2661–2733, 1998.
- [8] K. C. Joseph and M. J. Joshi, "The study of different parameters affecting Liesegang ring formation during the growth of calcium hydrogen phosphate dihydrate crystals," *Indian Journal of Physics*, vol. 76, pp. 159–163, 2002.

- [9] V. S. Joshi and M. J. Joshi, "FTIR spectroscopic, thermal and growth morphological studies of calcium hydrogen phosphate dihydrate crystals," *Crystal Research and Technology*, vol. 38, no. 9, pp. 817–821, 2003.
- [10] C. Y. C. Pak, K. Rodgers, J. R. Poindexter, and K. Sakhaee, "New methods of assessing crystal growth and saturation of brushite in whole urine: effect of pH, calcium and citrate," *Journal of Urology*, vol. 180, no. 4, pp. 1532–1537, 2008.
- [11] A. E. Krambeck, S. E. Handa, A. P. Evan, and J. E. Lingeman, "Brushite stone disease as a consequence of lithotripsy?" *Urological Research*, vol. 38, no. 4, pp. 293–299, 2010.
- [12] S. Mandel and A. C. Tas, "Brushite ( $\text{CaHPO}_4 \cdot 2\text{H}_2\text{O}$ ) to octacalcium phosphate ( $\text{Ca}_8(\text{HPO}_4)_2(\text{PO}_4)_4 \cdot 5\text{H}_2\text{O}$ ) transformation in DMEM solution at  $36.5^\circ\text{C}$ ," *Material Science and Engineering C*, vol. 30, no. 2, pp. 245–254, 2010.
- [13] W. F. Neuman, T. Y. Toribara, and B. J. Mulryan, "Synthetic hydroxyapatite crystals I. Sodium and potassium fixation," *Archives of Biochemistry and Biophysics*, vol. 98, no. 3, pp. 384–390, 1962.
- [14] C. Y. Pak, E. D. Eanes, and B. Ruskin, "Spontaneous precipitation of brushite in urine: evidence that brushite is the nidus of renal stones originating as calcium phosphate," *Proceedings of the National Academy of Sciences of the United States of America*, vol. 68, no. 7, pp. 1456–1460, 1971.
- [15] T. K. Anee, M. Palanichamy, M. Ashok, N. Meenakshi Sundaram, and S. N. Kalkura, "Influence of iron and temperature on the crystallization of calcium phosphates at the physiological pH," *Materials Letters*, vol. 58, no. 3–4, pp. 478–482, 2004.
- [16] N. Temizel, G. Giriskan, and A. C. Tas, "Accelerated transformation of brushite to octacalcium phosphate in new biomineralization media between  $36.5^\circ\text{C}$  and  $80^\circ\text{C}$ ," *Materials Science and Engineering C*, vol. 31, no. 5, pp. 1136–1143, 2011.
- [17] K. Rajendran and C. Dale Keefe, "Growth and characterization of calcium hydrogen phosphate dihydrate crystals from single diffusion gel technique," *Crystal Research and Technology*, vol. 45, no. 9, pp. 939–945, 2010.
- [18] M. P. Binitha and P. P. Pradyumnan, "Dielectric property studies of biologically compatible brushite single crystals used as bone graft substitute," *Journal of Biomaterials and Nanobiotechnology*, vol. 4, pp. 119–122, 2013.
- [19] A. R. Patel and A. Venkateswara Rao, "Crystal growth in gel media," *Bulletin of Materials Science*, vol. 4, no. 5, pp. 527–548, 1982.
- [20] N. Srinivasan and S. Natarajan, "Growth of some urinary crystals and studies on inhibitors and promoters. I. Standardisation of parameters for crystal growth and characterization of crystals," *Indian Journal of Physics*, vol. 70, pp. 563–568, 1996.
- [21] G. R. Sivkumar, E. K. Girija, S. Narayana Kalkura, and C. Subramanian, "Crystallization and characterization of calcium phosphates: brushite and monetite," *Crystal Research and Technology*, vol. 33, no. 2, pp. 197–205, 1997.
- [22] J. Ouyang, S. Deng, X. Li, Y. Tan, and B. Tieke, "Effects of temperature and sodium carboxylate additives on mineralization of calcium oxalate in silica gel systems," *Science in China B*, vol. 47, no. 4, pp. 311–319, 2004.
- [23] T. Bretherton and A. Rodgers, "Crystallization of calcium oxalate in minimally diluted urine," *Journal of Crystal Growth*, vol. 192, no. 3–4, pp. 448–455, 1998.
- [24] K. C. Joseph, B. B. Parekh, and M. J. Joshi, "Inhibition of growth of urinary type calcium hydrogen phosphate dihydrate crystals by tartaric acid and tamarind," *Current Science*, vol. 88, no. 8, pp. 1232–1238, 2005.
- [25] B. B. Parekh and M. J. Joshi, "Crystal growth and dissolution of brushite crystals by different concentration of citric acid solutions," *Indian Journal of Pure and Applied Physics*, vol. 43, no. 9, pp. 675–678, 2005.
- [26] C. Sekar and K. Suguna, "Effect of  $\text{H}_3\text{PO}_4$  reactant and NaF additive on the crystallization and properties of brushite," *Advanced Material Letters*, vol. 2, no. 3, pp. 227–232, 2011.
- [27] H. Lim, A. Kassim, N. Huang, P. Khiewc, and W. Chiu, "Three-dimensional flower-like brushite crystals prepared from high internal phase emulsion for drug delivery application," *Colloids and Surfaces A*, vol. 345, no. 1–3, pp. 211–218, 2009.
- [28] A. R. Kumar and S. Kalainathan, "Effect of magnetic field in the microhardness studies on calcium hydrogen phosphate crystals," *Journal of Physics and Chemistry of Solids*, vol. 71, no. 10, pp. 1411–1415, 2010.
- [29] B. B. Parekh, M. J. Joshi, and A. D. B. Vaidya, "Modification of gel technique for micro-crystals of biomaterials: in situ growth and dissolution studies," *Current Science*, vol. 93, no. 3, pp. 373–378, 2007.
- [30] H. K. Henisch, *Crystals in Gels & Liesegang Rings*, Cambridge University Press, Cambridge, UK, 1988.
- [31] G. Madhurambal, R. Subha, and S. C. Mojumdar, "Crystallization and thermal characterization of calcium hydrogen phosphate dihydrate crystals," *Journal of Thermal Analysis and Calorimetry*, vol. 96, no. 1, pp. 73–76, 2009.
- [32] J. J. de Yoreo and P. Vekilov, "Principles of crystal nucleation and growth," *Crystal Growth*, vol. 35, pp. 24–30, 2008.
- [33] S. M. Arifuzzaman and S. Rohani, "Experimental study of brushite precipitation," *Journal of Crystal Growth*, vol. 267, no. 3–4, pp. 624–634, 2004.
- [34] P. V. Dalal, K. B. Saraf, and S. Shah, "Growth of barium oxalate crystals in agar-agar gel and their characterization," *Crystal Research and Technology*, vol. 44, no. 1, pp. 36–42, 2009.
- [35] P. V. Dalal and K. B. Saraf, "Growth and study of barium oxalate single crystals in agar gel," *Bulletin of Materials Science*, vol. 29, no. 5, pp. 421–425, 2006.
- [36] B. M. Borah, H. Lakshmi, and G. Das, "Biomimetic modulation of crystal morphology using gel: from nano to micron-scale architectures," *Materials Science and Engineering C*, vol. 28, no. 7, pp. 1173–1182, 2008.
- [37] Joint Committee for Powder Diffraction Standards (JCPDS) Reference Card Number 001-0395.
- [38] Joint Committee for Powder Diffraction Standards (JCPDS) Reference Card Number 009-0077.
- [39] R. L. Frost and S. J. Palmer, "Thermal stability of the 'cave' mineral brushite  $\text{CaHPO}_4 \cdot 2\text{H}_2\text{O}$ —mechanism of formation and decomposition," *Thermochimica Acta*, vol. 521, no. 1–2, pp. 14–17, 2011.



